Competition between Peroxy Acid Oxygens as Hydrogen Bond Acceptors in B3LYP Transition Structures for Epoxidations of Allylic Alcohols with Peroxyformic Acid

Mauro Freccero,[†] Remo Gandolfi,[†] Mirko Sarzi-Amadè,*[,†] and Augusto Rastelli[‡]

Dipartimento di Chimica Organica, Università di Pavia, V.le Taramelli 10, 27100 Pavia, Italy, and Dipartimento di Chimica, Università di Modena, Via Campi 183, 41100 Modena, Italy

Received August 25, 1998

The transition structures (TSs) for the epoxidation of 2-propen-1-ol and 2-cyclobuten-1-ol with peroxyformic acid have been located with the B3LYP method using three basis sets (i.e., 6-31G*, 6-311G**, and 6-311+G**). Syn attacks on these alcohols by peroxy acid lead to syn TSs in which hydrogen bonding is operative. The allylic OH group always acts as hydrogen-bond donor while either the carbonyl oxygen or the peroxo oxygens of the peroxy acid can play the role of hydrogen-bond acceptors. In the case of propenol, the two syn TSs (O−C−C═C dihedral angles: 135.0° and 16.0°, respectively) with the peroxo oxygens involved in hydrogen bonding have free enthalpies comparable with those of their counterparts (O−C−C═C dihedral angles: 134.0° and 16.3°, respectively) with hydrogen bonding to carbonyl oxygen. Basis set extension as well as electrostatic solvation effects favor the former TSs over the latter ones. In the case of cyclobutenol the syn TS (O−C−C═C dihedral angle = 124.2°) with hydrogen bonding to peroxo oxygens is significantly more stable (by ≥1.8 kcal/mol^{-1}) than the corresponding TS (O−C−C═C dihedral angle = 128.0°) with carbonyl oxygen involved in hydrogen bonding. Anti TSs are inherently less stable than syn TSs but this difference is strongly reduced in solution. The Sharpless qualitative TS model for peroxy acid epoxidation of allyic alcohols is discussed in the light of computational data.

Introduction

Peroxy acid epoxidation of alkenes plays a very important role in organic synthesis as it provides versatile intermediates for the preparation of functionalized organic molecules.[1] Very recent theoretical investigations established that the S_N2-like nucleophilic attack by the ethylene π bond to the peroxo system of peroxyformic acid (PFA) occurs with synchronous C- - -O bond formation in a "spiro-butterfly" process. The plane of planar intramolecularly hydrogen-bonded peroxy acid is oriented at 90° to the C═C bond axis while the 1,4-hydrogen shift in the acid moiety is still at a very early stage.[2]

The peroxy acid attack to diastereotopic faces of carbon−carbon double bonds can be efficiently driven by stabilizing hydrogen-bonding interactions involving allylic OH substituent on the olefin as hydrogen-bond donor and the peroxy acid oxygens as hydrogen-bond acceptors.[3] This syn-OH orienting effect greatly improves the synthetic potentiality of peroxy acid epoxidation. Thus, there is a real need to have a transition structure model that accounts for this interaction as accurately as possible. Organic chemists have advanced transition structures (TSs) that feature the involvement of either the distal (e.g., **A** and **B**) or proximal (e.g., **C**) (Figure 1) peroxo oxygen for the epoxidations of both acyclic and cyclic alcohols.[3a,4] In particular, the planar butterfly TS **A**, advanced several years ago by Henbest et al.,[5] has more recently been replaced by the spiro TS **B**.[3a] The transition structure **C** was proposed later by Sharpless (in order to explain facial diastereoselectivities in the epoxidation of allylic alcohols)[6] and has been widely accepted by organic chemists.[3a] In this model, the hydrogen bonding involves only the proximal peroxo oxygen in an exo spiro TS (i.e., the dihedral angle between the peroxy acid plane and the double bond plane is ∼90°) with the plane of the peroxy acid moiety oriented at ∼60° to the C═C bond axis (see **D**). Sharpless stressed that this geometrical array orients the front side lone pair to efficiently hydrogen bond with the allylic OH group while at the same time the second lone pair can interact favorably with the π* orbital of the olefin (see **F**).

Researchers were well aware that hydrogen bonding could also involve the peroxy acid carbonyl oxygen,[4a,5] instead of peroxo oxygens, as hydrogen-bond acceptor but to date there has not been any claim of experimental data supporting this hypothesis. However, it might also be that the engagement of carbonyl oxygen in the intramolecular hydrogen bond could have led researchers to overlook this possibility.

* To whom correspondence should be addressed. Tel: +39 382 507668. Fax: +39 382 507323. E-mail: nmr@chifis.unipv.it.

† Università di Pavia.

‡ Università di Modena.

(1) Schwesinger, J. W.; Bauer, T. Diastereoselective Epoxidation. In *Stereoselective Synthesis*; Helmchem, G., Hoffmann, R. W., Mulzer, J., Schaumann, E., Eds.; Houben Weyl Thieme Stuttgart: New York, 1995; Vol. E21e, p 4599.

(2) (a) Singleton, D. A.; Merrigan, S. R.; Jian Liu; Houk, K. N. *J. Am. Chem. Soc.* **1997**, *119*, 3385. (b) Houk, K. N.; Liu, J.; DeMello, N. C.; Condroski, K. R. *J. Am. Chem. Soc.* **1997**, *119*, 10147. (c) Bach, R. D.; Canepa, C.; Winter J. E.; Blanchette, P. E. *J. Org. Chem.* **1997**, *62*, 5191. (d) Bach, R. D.; Glukhovtsev, M. N.; Gonzales, C.; Marquez, M.; Estevez, C. M.; Baboul, A. G.; Schlegel, H. B. *J. Phys. Chem. A* **1997**, *101*, 6092. (e) Bach, R. D.; Glukhovtsev, M. N.; Gonzales, C. *J. Am. Chem. Soc.* **1998**, *120*, 9902.

(3) (a) Hoveyda, A. H.; Evans, D. A.; Fu, G. C. *Chem. Rev.* **1993**, *93*, 1307. (b) For an excellent treatise on hydrogen bonding, see: Jeffrey, J. A. *Introduction to hydrogen bonding*; University Press: Oxford, 1997.

(4) (a) Kocovsky, P.; Stary, I. *J. Org. Chem.* **1990**, *55*, 3236 and references therein. (b) Adam, W.; Smerz, A. K. *J. Org. Chem.* **1996**, *61*, 3506.

(5) Hembest, H. B.; Wilson, R. A. L. *J. Chem. Soc.* **1959**, 1958.

(6) Sharpless, K. B.; Verhoeven, T. R. *Aldrichim. Acta* **1979**, *12*, 63.

10.1021/jo981743u CCC: $18.00
Published on Web 05/04/1999

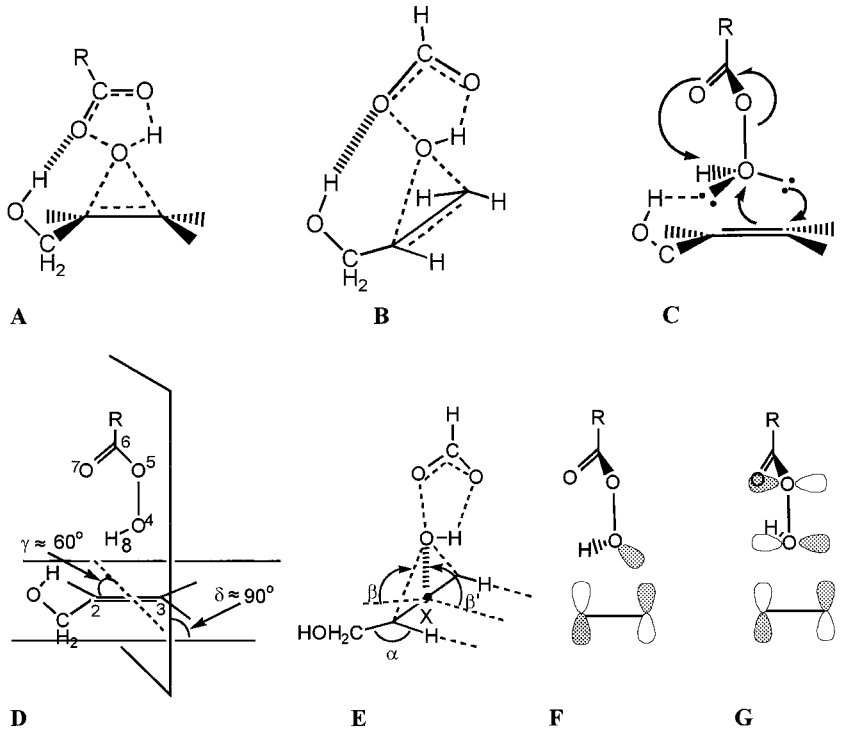

Figure 1. Qualitative models (**C** and **D** illustrate the Sharpless hypothesis) for transition structures of the epoxidation of allylic alcohols with peroxy acids. Schematic descriptions of the electron back-donation ($HOMO_{peroxyformic} - LUMO_{alkene}$) from peroxy acid to alkene (**F** and **G**).

The control of facial selectivity by intramolecular hydrogen bond has also been observed in the related epoxidation of allylic alcohols by dimethyldioxirane.[7] The stereocontrol closely resembles that of peroxy acid reactions but is generally lower, at least in the case of acyclic alcohols. This trend was explained by assuming that in both reactions the distal peroxo oxygen accepts the hydrogen bond, but the dioxirane peroxo bond is much less polarized in the transition state than the peroxy acid peroxo bond with a consequently considerably less effective interaction in the former than in the latter reaction.[4b]

On the computational side, several authors have recently demonstrated that peroxo oxygens can efficiently play the role of hydrogen-bond acceptor (in both intermolecular and intramolecular interactions) in the dioxirane epoxidation.[8−10a]

Thus, in the light of the above discussion, the very recent result by Bach et al. is very interesting. In striking contrast to the "qualitative" models **A**−**C**, these authors located two TSs (at the B3LYP/6-311G** level) for the epoxidation of 2-propen-1-ol with peroxyformic acid (PFA) with carbonyl oxygen as hydrogen-bond acceptor.[11] These authors did not explicitly comment whether alternative competing reaction pathways, which pass through TSs in which the peroxo oxygens act as hydrogen-bond acceptors, can be operative or not in this reaction. This question is of particular relevance for researchers who are interested in predicting the stereochemical outcome of peroxy acid epoxidation of allylic (and homoallylic) alcohols on the basis of simple qualitative models.

The above considerations suggest the importance of a reliable definition of the relative energy and the geometry details of the transition structures of peroxy acid epoxidations of allylic alcohols. Moreover, it is important to assess to what extent the geometrical details of the Sharpless model, i.e., **C**, can be retained in a useful and simple TS model for peroxy acid epoxidation of the same substrates.

To start to answer these questions we have reinvestigated at a good theory level (B3LYP method with 6-31G*, 6-311G** and, for some structures, 6-311+G** basis sets) the reaction of PFA with 2-propenol and have extended our study to the epoxidation of a cyclic allylic alcohol, i.e., 2-cyclobuten-1-ol.

Computational Methods

It is well-known that the relative magnitude of hydrogen-bonding interactions are not easy to reproduce by all theoretical methods. However, DFT methods, which include electron correlation, lend themselves as promising methods to study these interactions.[12] We carried out the complete set of calculations for the reactions under study with density functional theory (DFT) using the Becke3-LYP functional[13,14] with the 6-31G* basis set as well as with a more flexible basis set with polarization function also on the hydrogen atoms, i.e., the 6-311G** basis set previously used by Bach et al.[11] Two competing TSs were also optimized at the B3LYP/6-311+G**

(7) Murray, R. W. *Chem. Rev.* **1989**, *89*, 1187.
(8) Miaskiewicz, K.; Smith, D. A. *J. Am. Chem. Soc.* **1998,** *120***,** 1872.
(9) Jenson, C.; Jian Liu; Houk, K. N.; Jorgensen, W. L. *J. Am. Chem. Soc.* **1997**, *119*, 12982.
(10) (a) Freccero, M.; Gandolfi, R.; Sarzi-Amadè M.; Rastelli, A *Tetrahedron* **1998**, *54*, 12323. (b) Freccero, M.; Gandolfi, R.; Sarzi-Amadè M.; Rastelli, A *Tetrahedron* **1998**, *54*, 6123. (c) Sharpless adopts a "rabbit-ear" representation of oxygen lone pairs (they occupy sp^3-hybrid atomic orbitals) while in **G** a MO description of lone pairs is used.
(11) Bach, R. D.; Estévez, C. M.; Winter J. E.; Glukhovtsev, M. N. *J. Am. Chem. Soc.* **1998**, *120*, 680.
(12) (a) Sim, F.; St-Amant, A.; Papai, I.; Salahub, D. R. *J. Am. Chem. Soc.* **1992**, *114*, 4391. (b) Caminati, W.; Moreschini, P.; Rossi, I.; Favero, P. G. *J. Am. Chem. Soc.* **1998**, *120*, 11148.
(13) Becke, A. D. *J. Chem. Phys.* **1993**, *98*, 1372.
(14) Lee, C.; Yang, W.; Parr, R. G. *Phys. Rev. B* **1988**, *37*, 785.

Table 1. Relative Free Enthalpies (G_{rel}), Bond Lengths (Angstroms), Angles (Degrees), OH Stretching Frequencies (ν_{OH}), and Dipole Moments (μ) of 2-Propen-1-ol (1a-e) and 2-Cyclobuten-1-ol (2a,c,d) Conformers at the B3LYP/6-311G Level[a]**

conformer	G_{rel} (kcal/mol)	C_1-C_2	$H-O-C_1-C_2$	$O-C_1-C_2-C_3$	ν_{OH} (cm^{-1})	μ (debye)
1a	0.06	1.330	−57.6	124.4	3817	1.54
1b	0.00	1.329	61.5	7.0	3814	1.54
1c	1.45	1.328	168.4	129.0	3836	1.66
1d	1.39	1.328	65.4	121.6	3826	1.64
1e	0.78	1.327	180.7	0.2	3853	1.86
2a	0.00	1.338	−43.4	123.4	3807	1.60
2c	1.66	1.337	−183.3	122.0	3821	1.59
2d	1.87	1.336	77.6	116.6	3826	1.49

[a] For B3LYP/6-31G* data see ref 10 and the Supporting Information.

Table 2. Bond Lengths (Angstroms), Angles (Degrees), Transition Mode, OH Stretching Frequency (ν_{OH}), Dipole Moment (μ), Electron Transfer, and Net Atomic Charges for the TSs of the PFA Epoxidation of 1 and 2 at the B3LYP/6-311G Level[a,b]**

parameter[c]	**3a**	**3b**	**4a**	**4b**	**5a**	**6a**	**7a**	**8a**	**9a**	**10a**
C_2-C_3	1.366	1.364	1.366	1.366	1.368	1.368	1.372	1.374	1.378	1.378
O_5-C_6	1.279	1.282	1.287	1.285	1.282	1.282	1.283	1.287	1.282	1.283
C_6-O_7	1.236	1.233	1.228	1.230	1.232	1.232	1.235	1.228	1.233	1.231
$H-O-C_1-C_2$	−73.3	87.6	−56.3	61.9	66.8	66.8	−54.4	−39.8	48.3	49.7
$O-C_1-C_2-C_3$	134.2	16.3	135.0	16.0	−111.8	−117.5	128.0	124.2	−121.1	−122.9
$X-O_4-O_5$	171.9	170.4	175.2	177.9	176.1	177.6	173.0	178.5	178.0	
$O_4-O_5-C_6-O_7$	3.5	3.7	0.3	0.2	0.6	0.1	2.2	0.3	0.2	0.1
$H_8-O_4-O_5-C_6$	15.9	14.7	0.6	0.3	1.2	0.6	10.6	0.7	0.3	0.7
$\lvert 180° - \alpha \rvert$	5.0	4.8	4.1	4.7	7.1	6.6	8.9	6.8	7.9	6.3
β	97.6	94.2	87.7	86.7	97.6	89.6	105.0	93.8	105.9	96.4
β'	87.3	89.4	96.3	98.0	89.5	96.2	83.7	92.8	81.8	89.7
γ	54.7	77.0	101.2	83.4	95.0	87.2	78.8	81.9	89.5	83.7
δ	86.9	84.3	83.2	91.2	91.1	87.7	83.3	85.5	89.1	86.0
transition mode (cm^{-1})	394	397	389	391	418	417	402	375	419	403
ν_{OH} (cm^{-1})	3678	3677	3773	3780	3818	3820	3679	3763	3802	3804
μ (debye)	3.12	2.48	3.18	2.58	3.51	3.68	2.81	3.10	4.03	3.74
electron tranfer[d]	0.27	0.29	0.27	0.31	0.29	0.29	0.25	0.29	0.29	0.30
net atomic charges[e]										
O_4	−0.27	−0.26	−0.26	−0.33	−0.26	−0.30	−0.26	−0.34	−0.26	−0.30
O_5	−0.41	−0.42	−0.43	−0.43	−0.43	−0.43	−0.41	−0.43	−0.44	−0.43
O_7	−0.60	−0.61	−0.58	−0.59	−0.60	−0.59	−0.60	−0.58	−0.60	−0.59

[a] O_4-H_8 bond length in TS **3**−**10** is in the range = 0.983−1.003 Å. [b] HCOOOH ground-state geometry: O_4-O_5, 1.441 Å; O_5-C_6, 1.341 Å; C_6-O_7, 1.201 Å; O_4-H_8, 0.981 Å; H−O−O−C and O−O−C−O = 0°; μ = 1.35 D. CHelpG (Mulliken) net atomic charges: O_4 = −0.34 (−0.21); O_5 = −0.21 (−0.14); O_7 = −0.49 (−0.34). [c] For numbering see **E** in Figure 1. For the meaning of α and β see the Computational Methods. [d] From olefin to PFA according to the CHelpG method. Electron-transfer according to Mulliken analysis is similar (~0.30). [e] CHelpG charges. Mulliken population analysis leads to a more balanced negative charge distribution: ca. −0.30 on both O_4 and O_5 and ca. −0.40 on O_7.

level in order to ascertain to what extent and in what direction a further improvement of the basis set will change the relative energy of TSs.

All calculations were performed with the Gaussian 94 suite of programs.[15] Critical points have been characterized by diagonalizing the Hessian matrixes calculated for the optimized structures. Energies and geometrical data of conformational minima of 2-propen-1-ol and 2-cyclobuten-1-ol are reported in Table 1. Transition structures have only one negative eigenvalue (first-order saddle points) with the corresponding eigenvector involving the expected formation of the two new oxirane bonds, the cleavage of the O_4-O_5, the lengthening of the $C_6=O_7$, and the shortening of the O_5-C_6 peroxy acid bonds (see **D** in Figure 1 for TS numbering). The transition mode imaginary frequencies (cm^{-1}) of the TSs are reported in Table 2. The search for TSs was limited to concerted transition structures; i.e., only restricted B3LYP methods have been used.

The geometries obtained with the three basis sets look very similar to each other so that we here report only the data at the B3LYP/6-311G** level (Cartesian coordinates of TSs located with the other two basis sets are available in the Supporting Information).

Forming bond lengths are reported in Figure 3, while in addition to α and β angles (**E**, Figure 1), the following angles are gathered in Table 2: (i) the torsional angles ($H-O-C_1-C_2$ and $O-C_1-C_2-C_3$) necessary to describe rotations about the $O-C_1$ and C_1-C_2 bonds; (ii) the $X-O_4-O_5$ angle, which allows one to evaluate the alignment of the axis of the π cloud with the breaking O_4- - -O_5 bond (X is a dummy atom placed at the center of the C_2-C_3 bond) (a value lower than 180° indicates that O_5 is bent toward the side of the C=O- - -H peroxy acid moiety); (iii) the $H_8-O_4-O_5-C_6$ and $O_4-O_5-C_6-O_7$ torsional angles related to out-of-plane distortion of the peroxy acid moiety; (iv) γ, the angle between the $O_4-O_5-C_6$ plane of the attacking peroxy acid and the $C_2=C_3$ bond axis (a value lower than 90° means that the C_6O_7 peroxy acid fragment is closer to C_2 than to C_3 (see **D**, Figure 1) as a result of rotation around the O_4- - -O_5 bond); and (v) δ, the dihedral angle between the $O_4-O_5-C_6$ plane of the attacking peroxy acid and the mean plane of the double bond moiety. A value larger (smaller) than 90° means that the peroxy acid plane is tilted away from (toward) the CH_2OH group.

A value of 90° for both γ and δ corresponds to a symmetrical spiro structure. It should be realized that the γ and δ angles practically also correspond to the angles between the mean PFA plane and, respectively, the $C_2=C_3$ bond axis and the $C_2=C_3$ plane in **4a**, **4b**, **5a**, **6a**, **8a**, **9a**, and **10a** (all these TSs exhibit a planar PFA moiety). However, this is not true for

(15) Gaussian 94: Frisch, M. J.; Trucks, G. W.; Schlegel, H. B.; Gill, P. M. W.; Johnson, B. G.; Robb, M. A.; Cheeseman, J. R.; Keith, T.; Peterson, G. A.; Montgomery, J. A.; Raghavachari, K.; Al-Laham, M. A.; Zakrzewski, V. G.; Ortiz, J. V.; Foresman, J. B.; Cioslowski, J.; Stefanov, B. B.; Nanayakkara, A.; Challacombe, M.; Peng, C. Y.; Ayala, P. Y.; Chen, W.; Wong, M. W.; Andres, J. L.; Replogle, E. S.; Gompert, R, Martin, R. L.; Fox, D. J.; Binkley, J. S.; Defrees, D. J.; Baker, J.; Stewart, J. P.; Head-Gordon, M.; Gonzales C.; Pople, J. A. Gaussian, Inc., Pittsburgh, PA, 1995.

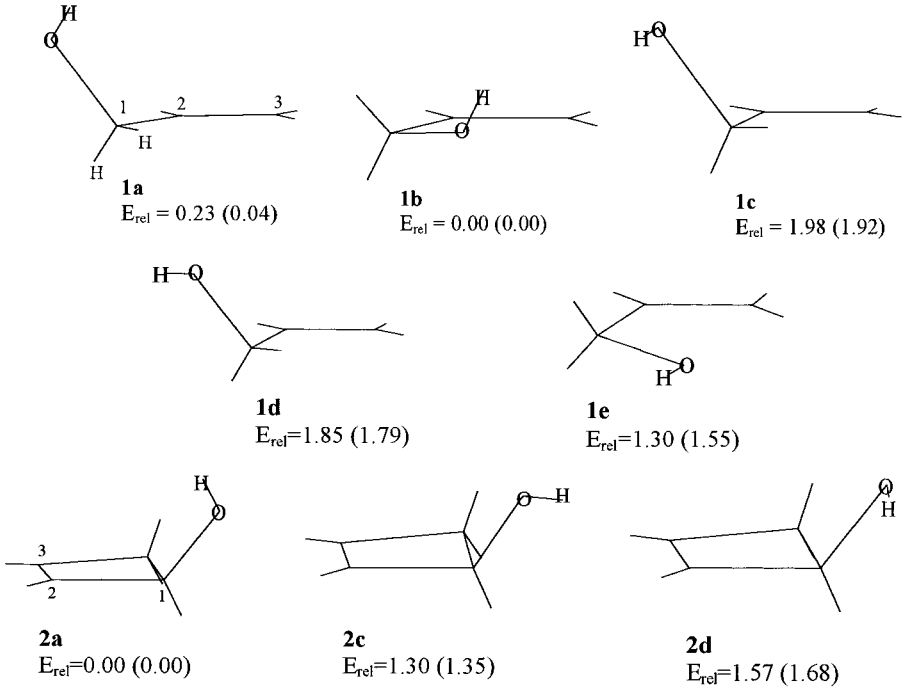

Figure 2. B3LYP conformational minima of 2-propen-1-ol (**1a**−**e**) and 2-cyclobuten-1-ol (**2a**,**c**−**d**) with their relative energies (kcal/mol) at the B3LYP/6-311G** (B3LYP/6-31G*) level.

Table 3. Relative Electronic Energies ($E^{\ddagger}_{rel}$), Enthalpies ($H^{\ddagger}_{rel}$), Entropies ($S^{\ddagger}_{rel}$), and Free Enthalpies [$G^{\ddagger}_{rel}$ (Gas Phase), $G^{\ddagger}_{sol,rel}$ (Solution)] for the Epoxidation of Propenol (TSs 3−6) and Cyclobutenol (TSs 7a−10a) at the B3LYP/6-31G* Level[a]

	3a	3b	4a	4b	5a	6a		7a	8a	9a	10a
$E^{\ddagger}_{rel}$	2.12	0.00	2.03	1.77	6.54	6.02	$E^{\ddagger}_{rel}$	1.15	0.00	6.20	4.43
$H^{\ddagger}_{rel}$	2.04	0.00	1.79	1.50	6.28	5.74	$H^{\ddagger}_{rel}$	1.39	0.00	6.16	4.39
$S^{\ddagger}_{rel}$	−0.10	0.00	1.92	2.29	5.07	4.70	$S^{\ddagger}_{rel}$	−1.47	0.00	1.92	1.57
$G^{\ddagger}_{rel}$	2.08	0.00	1.22	0.82	4.77	4.34	$G^{\ddagger}_{rel}$	1.80	0.00	5.57	3.92
$G^{\ddagger}_{sol,rel}$[b,c]	1.60	0.00	0.41	0.08	3.24	2.69	$G^{\ddagger}_{sol,rel}$[b,c]	2.33	0.00	4.80	3.12
$G^{\ddagger}_{sol,rel}$[b,d]	1.14	0.00	−0.19	−0.43	1.87	1.22	$G^{\ddagger}_{sol,rel}$[b,d]	2.69	0.00	3.99	2.29

[a] Energies in kcal/mol and entropies in cal/mol K; harmonic approximation assumed; standard state (298 K) of the molar concentration scale. Activation parameters, evaluated with respect to the corresponding propenol conformer **1a** (**1b**), for **3a** (**3b**): $\Delta E^{\ddagger} = 9.83$ (7.75), $\Delta H^{\ddagger} = 10.57$ (8.63), $\Delta S^{\ddagger} = -33.3$ (−32.5), $\Delta G^{\ddagger} = 20.52$ (18.31), $\Delta G^{\ddagger}_{sol,C_6H_6} = 20.30$ (18.54), and $\Delta G^{\ddagger}_{sol,CH_2Cl_2} = 20.04$ (18.77). Activation parameters, evaluated with respect to cyclobutenol conformer **2a**, for **8a**: $\Delta E^{\ddagger} = 8.75$, $\Delta H^{\ddagger} = 9.19$, $\Delta S^{\ddagger} = -30.83$, $\Delta G^{\ddagger} = 18.39$, $\Delta G^{\ddagger}_{sol,C_6H_6} = 17.94$ and $\Delta G^{\ddagger}_{sol,CH_2Cl_2} = 17.65$. [b] Electrostatic solvent effect is introduced by using the Tomasi model at the B3LYP/6-31G* level. For AMSOL data ($\epsilon = 2.02$) see ref 26. [c] In C_6H_6 ($\epsilon = 2.3$). [d] In CH_2Cl_2 ($\epsilon = 8.9$).

Table 4. Relative Electronic Energies ($E^{\ddagger}_{rel}$), Enthalpies ($H^{\ddagger}_{rel}$), Entropies ($S^{\ddagger}_{rel}$) and Free Enthalpies [$G^{\ddagger}_{rel}$ (Gas Phase), $G^{\ddagger}_{sol,rel}$ (solution)] for the Epoxidation of Propenol (TSs 3−6) and Cyclobutenol (TSs 7a−10a) at the B3LYP/6-311G Level[a]**

	3a	3b	4a	4b	5a	6a		7a	8a	9a	10a
$E^{\ddagger}_{rel}$	2.15	0.00	1.67	1.16	6.25	5.57	$E^{\ddagger}_{rel}$	1.71	0.00	6.43	4.30
$H^{\ddagger}_{rel}$	2.13	0.00	1.57	1.01	6.14	5.43	$H^{\ddagger}_{rel}$	1.86	0.00	6.33	4.27
$S^{\ddagger}_{rel}$	0.03	0.00	1.75	2.24	4.45	4.67	$S^{\ddagger}_{rel}$	−0.92	0.00	2.48	1.29
$G^{\ddagger}_{rel}$	2.12	0.00	1.05	0.34	4.81	4.03	$G^{\ddagger}_{rel}$	2.13	0.00	5.59	3.89
$G^{\ddagger}_{sol,rel}$[b,c]	1.64	0.00	0.24	−0.40	3.28	2.38	$G^{\ddagger}_{sol,rel}$[b,c]	2.66	0.00	4.82	3.09
$G^{\ddagger}_{sol,rel}$[b,d]	1.18	0.00	−0.36	−0.91	1.91	0.91	$G^{\ddagger}_{sol,rel}$[b,d]	3.02	0.00	4.01	2.26

[a] See footnote a in Table 3. Activation parameters for **3a** (**3b**): $\Delta E^{\ddagger} = 10.73$ (8.81), $\Delta H^{\ddagger} = 11.26$ (9.43), $\Delta S^{\ddagger} = -32.77$ (−32.03), $\Delta G^{\ddagger} = 21.04$ (18.98), $\Delta G^{\ddagger}_{sol,C_6H_6} = 20.82$ (19.21), $\Delta G^{\ddagger}_{sol,CH_2Cl_2} = 20.56$ (19.44). Activation parameters for **8a**: $\Delta E^{\ddagger} = 9.10$, $\Delta H^{\ddagger} = 9.41$, $\Delta S^{\ddagger} = -30.39$, $\Delta G^{\ddagger} = 18.47$, $\Delta G^{\ddagger}_{sol,C_6H_6} = 18.02$, and $\Delta G^{\ddagger}_{sol,CH_2Cl_2} = 17.73$. [b−d] As in Table 3.

TSs with out-of-plane distorted PFA moiety as in **3a**, **3b**, and **7a** (in which both H_8 and O_7 are rotated out of the $O_4-O_5-C_6$ plane by ≥11° and ≥2°, respectively).

To produce theoretical activation parameters, vibrational frequencies in the harmonic approximation were calculated for all the optimized structures and used, unscaled,[16] to compute the zero point energies, their thermal corrections, the vibrational entropies, and their contributions to activation enthalpies, entropies, and free enthalpies (Tables 3 and 4).

The contribution of electrostatic solvent effects to the activation free enthalpy of the reactions under study were calculated via the self-consistent reaction field (SCRF) using the Tomasi model (interlocking spheres) by single-point calculations (i.e., with unrelaxed gas-phase geometries of reactants and TSs) at the B3LYP/6-31G* level (Tables 3 and 4) by using the dielectric constants of benzene ($\epsilon = 2.3$) and of dichloromethane ($\epsilon = 8.9$).[17] The AMSOL method ($\epsilon = 2.02$) allowed us to confirm the data of the Tomasi model in the less polar solvent.

(16) Rastelli, A.; Bagatti, M.; Gandolfi, R. *J. Am. Chem. Soc.* **1995**, *117*, 4965.

(17) Tomasi, J.; Persico, M.*Chem. Rev.* **1997**, *94*, 2027.

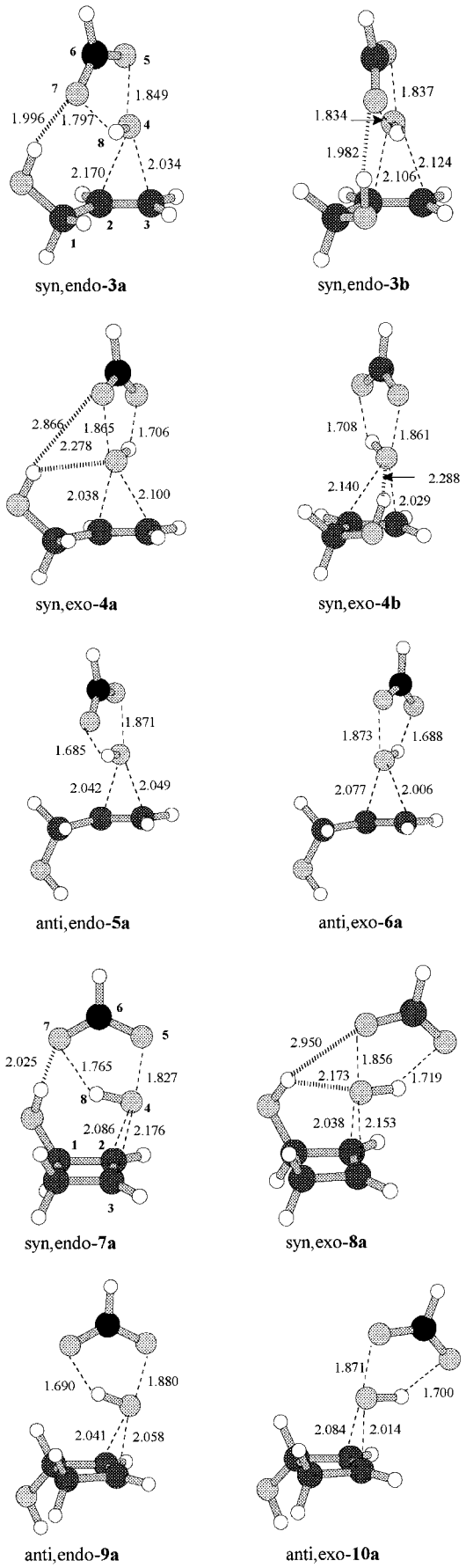

Figure 3. Optimized (B3LYP/6-311G**) transition structures (bond lengths in Å) for epoxidation of 2-propen-1-ol (**3**−**6**) and 2-cyclobuten-1-ol (**7a**−**10a**) with peroxyformic acid.

Results

Conformers of 2-Propen-1-ol and 2-Cyclobuten-1-ol. We have already reported the conformational profile of 2-propen-1-ol (**1**) calculated at the B3LYP/631G* level.[10a] In addition, its B3LYP/6-311G** potential energy surface exhibits five minima (E_{rel} in Figure 2 and G_{rel} in Table 1). At both levels conformers **1a** and **1b** are definitely more stable than the other three (i.e., **1c**−**e**). In the two most stable conformers the hydroxylic hydrogen weakly hydrogen bonds the π system with a resultant lower O−H stretching frequency in comparison with that in the other conformers (Table 1).

Likewise, the hydrogen bonded conformer **2a** of 2-cyclobuten-1-ol (**2**) is more stable than **2c**,**d** (Figure 2 and Table 1).

In **1a**, **1b**, and **2a**, the hydroxylic hydrogen is properly oriented to be involved, without a deep molecular structure reorganization, in hydrogen bonding with the peroxy acid from the very beginning of a syn attack.

Transition Structures for the Reactions of 1 and 2 with PFA. All the first-order saddle points located for the reaction of PFA with **1** and **2**, respectively, feature a spiro-butterfly structure (Figure 3 and Table 2, only the B3LYP/6-311G** geometries are reported). All of the TSs are characterized by low asynchrony (<0.140 Å) in C- - -O bond formation and by a very small lengthening of the O_4-H_8 bond. The alkene fragment has only slightly been perturbed as shown, for example, by the small elongation (Table 2) as well as by the small out-of-planarity deformation of the double bond ($|180° - \alpha| \approx 4-9°$, Table 2). The forming oxirane plane is, as a rule, inclined to the opposite side of the C═O- - -H peroxy acid moiety no matter whether this moiety is endo or exo[18] oriented with respect to the olefin substituent(s) (i.e., $\beta > \beta'$ in TSs endo and $\beta' > \beta$ in TSs exo, Table 2). This inclination is particularly pronounced in endo TS of **2** in order to lessen steric interactions.

Another feature shared by all transition structures located in this study is represented by the sizable electron density transfer from the allylic alcohols to PFA (~0.3 electron, Table 2) in accord with an electrophilic attack by PFA on the olefin. The negative net atomic charge (CHelpG charges, Table 2) located on the distal peroxy acid peroxo oxygen (ca. −0.42) is slightly larger than that on the proximal one (ca. −0.30). Charge transfer and peroxo bond polarization given by calculations for PFA epoxidation are thus very similar to those found for dimethyldioxirane epoxidation[10a] in contrast to the previous suggestion of a lower O- - -O polarization for the latter than for the former reaction.[4b] Noteworthy is the observation that in these TSs the highest negative net charge is observed on the carbonyl oxygen (ca. −0.60).

For the reaction of propenol with PFA we located five syn transition structures (only the four most relevant, i.e., **3a**−**4b**, are reported here, Figure 3).[19] They can be described as deriving from syn attacks (i.e., on the olefinic face syn to the OH group) on the two most stable propenol conformers **1a** and **1b**, with the peroxy acid endo (**3a** and **3b**) and exo (**4a** and **4b**) oriented with respect to the olefin substituent.

In *syn*,*endo*-**3a** and *syn*,*endo*-**3b**, which are the TSs located by Bach et al., hydrogen bonding involves the

(18) The endo (exo) descriptor is used for TSs in which the PFA C_6═O_7- - -H_8 moiety and the olefin substituent with the highest Cahn−Ingold−Prelog priority are on the same (opposite) side.

allylic OH group and the peroxy acid carbonyl oxygen.[20] This hydrogen-bonding certainly benefits from the higher basicity of the carbonyl oxygen[11] with respect to that of the peroxo oxygens, but to attain and strengthen this interaction, the peroxy acid hydrogen suffers a sizable out-of-plane distortion ($H_8-O_4-O_5-C_6 = 16°$ in *syn,endo*-**3a** and 15° in *syn,endo*-**3b** vs 0° in PFA) (Table 2). In fact, the peroxy acid prefers a planar conformation as shown by its planar ground-state structure and by the observation that in all other TSs it adopts a planar atom array (Table 2). In **3a** and **3b** there is a rotation, around the breaking O_4- - -O_5, not only of the O_4-H_8 bond away from the allylic OH group but also of the $C_6=O_7$ bond toward this group. In fact, in these TSs also the carbonyl oxygen is rotated out of the $O_4-O_5-C_6$ plane by ~4° (see $O_4-O_5-C_6-O_7$ in Table 2).

In both **3a** and **3b** the trajectory of approach between the reactants deviates somewhat from the ideal one (i.e., the one that maximizes stabilizing orbital interactions) once again in order to bring the carbonyl oxygen closer the OH group. This, however, leads to a worse alignment between the π orbital axis and the breaking O_4- - -O_5 bond as documented by $X-O_4-H_8$ (~88−90°) and $X-O_4-O_5$ (~172°) (X is a dummy atom placed at the center of the C_2-C_3 bond; see **E** in Figure 1) angles that are smaller than those (~94° and ~177°, respectively) observed in TSs whose geometry more closely reflect orbital interactions (i.e., in anti TSs as well as in TSs of ethene and propene PFA epoxidations).[2,21]

Syn,exo attacks on **a** and **b** propenol conformers, respectively, give rise to *syn,exo*-**4a** and *syn,exo*-**4b**, where the peroxo oxygens are the hydrogen-bond acceptor centers. In *syn,exo*-**4b** only the proximal oxygen is heavily involved [O_5 seems to be too far (ca. 3.2 Å) for sizeable hydrogen bonding] while in *syn,exo*-**4a** aside from the proximal oxygen (O_4, net charge −0.26) also the distal one (O_5, net charge −0.43) seems to participate in this interaction. It should be noticed that there is not any significant out-of-plane distortion of the peroxy acid moiety in these two TSs ($H_8-O_4-O_5-C_6$ and $O_4-O_5-C_6-O_7 < 1°$, Table 2). TS **4a** exhibits a slight rotation of the peroxy acid plane around the O_4- - -O_5 bond (see $\gamma = 101°$, Table 2) and a shortening of the O_4- - -C_2 forming bond. As a result, both peroxo oxygens get closer to the OH group and also the distal one can be involved, to some extent, in hydrogen bonding. Notice that O_5 exhibits a better alignment than O_4 for this interaction ($O-H---O_4$ angle = 122.6° vs $O-H---O_5$ angle = 163.6).[3b]

Comparing the geometries of **3a** and **3b** with those of **4a** and **4b**, we can conclude that (i) the former TSs are certainly favored over the latter ones by a stronger hydrogen bonding [as also testified by the lower OH (allylic) stretching frequency in **3a** and **3b** as compared to **4a** and **4b**; Table 2] but (ii) disfavored by geometry distortion in the PFA fragment, by an approach trajectory between the reactants which allows a less efficient orbital interaction and, being **3a** and **3b** endo TSs, by a higher steric crowding.

Examples of TSs whose geometry is not perturbed by hydrogen bonding are provided by the six anti TSs (only two, that is *anti,endo*-**5a** and *anti,exo*-**6a**, are here reported):[22] steric congestion is no doubt the underlying reason of the higher (0.5−0.7 kcal/mol) energy of *endo*-**5a** in comparison with *exo*-**6a**.

It is well known that convergence of molecular geometry with respect to the method is obtained considerably more readily than is convergence for energies. For transtion structures under study, not only, as expected, the absolute energy values but also the relative energy values are basis set dependent.[23] At the B3LYP/6-31G* level, the potential energy of TS **3b** is definitely lower than that of the other TSs even if differences are far from being dramatic. The stability ranking of the syn TSs is as follows: *endo*-**3b** > *exo*-**4b** > *exo*-**4a** > *endo*-**3a** (E_{rel} = 0.00, 1.77, 2.03 and 2.12 kcal/mol, respectively; Table 3). As quoted above, hydrogen bonding in **3a** and **3b** is stronger than that in **4a** and **4b**. However, the decrease in the electronic energy (as well as in the enthalpy) brought about by this interaction is paralleled, as a result of more organized TSs, by an increase in entropy that now favors **4a** and **4b** by ~2 eu over **3a** and **3b**.[24] At the free enthalpy level (gas phase), **3b** (0.00 kcal/mol) continues to be the most stable TS, but its favor over **4b** (0.82 kcal/mol) and **4a** (1.22 kcal/mol) is now substantially reduced while that over **3a** (2.08 kcal/mol) does not change.

These energy trends are reproduced by the higher basis set, i.e., B3LYP/6-311G** (Table 4). Interestingly, improving the basis set adds a stabilization of ~0.2−0.5 kcal/mol to TSs with hydrogen bond to peroxo oxygens (**4a** and **4b**) relative to those with hydrogen bond to carbonyl oxygen (**3a** and **3b**). At this calculation level, the relative potential energies (free enthalpies) for *endo*-**3b**, *exo*-**4b**, *exo*-**4a**, and *endo*-**3a** are as follows: 0.00 (0.00), 1.16 (0.34), 1.67 (1.05), and 2.15 (2.12) kcal/mol.

Moreover, introduction of diffuse functions (B3LYP/6-311+G**) further decreases the difference in potential energy between **3b** (0.00 kcal/mol) and **4b** (0.19 kcal/mol) and brings about reversal in their relative free enthalpies [*exo*-**4b** (−0.61 kcal/mol) is now more stable than *endo*-**3b** (0.00 kcal/mol)].[25]

Potential energies and free enthalpies of TSs originating from anti attacks, such as *anti,endo*-**5a** and *anti,exo*-

(19) (a) Aside from *endo*-**3a** and *endo*-**3b**, we located a further syn,-endo TS. However, in this TS the hydrogen-bonding interaction involves the two peroxo oxygens (instead of the carbonyl oxygen as in the endo TS **3a** and **3b**) and the $C_6=O_7$- - -H_8 fragment is rotated away from the OH (allylic) group ($\gamma = 121°$). At the B3LYP/6-31G* level, the electronic energy (free enthalpy) of this TS is higher by 3.72 kcal/mol (2.89 kcal/mol) with respect to **3b**. (b) To date we were not able to locate, for systems under study, TSs in which the peroxy acid is the hydrogen bond donor and the allylic alcohol the hydrogen bond acceptor (this interaction has been advanced as the facial selectivity controlling factor in the epoxidation with highly acidic peroxy acids by McKittrick, B. A.; Ganem, B. *Tetrahedron Lett.* **1985**, *26*, 4895); however, see: Fehr, C. *Angew. Chem., Int. Ed. Engl.* **1998**, *37*, 2407.

(20) These authors reported[11] the electronic activation energy for their TSs (our **3a** and **3b**) without specifying with respect to which conformer it was calculated. Their values can be reproduced by using as reactant the propenol conformer **1e**.

(21) Freccero, M.; Gandolfi, R.; Sarzi-Amadè M.; Rastelli, A. Unpublished results.

(22) The geometries of the three anti,exo and as well as of the three anti,endo TSs differ from each other significantly only in the $H-O-C_1-C_2$ dihedral angle. Thus, both exo and endo TSs exhibit three conformations that roughly correspond to the **a**, **c**, and **d** conformations of the starting allylic alcohols.

(23) However, it must be stressed that B3LYP calculations, with both the 6-31G* and 6-311G** basis set, give $\Delta G^{\ddagger}$ values that are in reasonable agreement with experimental data. In fact, the activation free enthalpies for TSs **3**−**4** ($\Delta G_{298}^{\ddagger} \approx 18-21$ kcal/mol, see Tables 3 and 4 and Supporting Information) and for **8a** (~18 kcal/mol) compare well with experimental data for epoxidation of 3-hydroxycyclohexene ($\Delta G_{278}^{\ddagger} \approx 19.7$ kcal/mol).[3]

(24) We will discuss in a forthcoming paper the problem of the lower reaction rate of allylic alcohols with respect to corresponding alkenes. Experimental data suggest that this observation is the result of adverse entropic factors that overcome favorable enthalpic factors.[3a]

6a, are much higher than those of syn TSs (Tables 3 and 4) with all calculation methods used.

But what about solvent effects? To get at least an idea of solvation effects on the relative TS energies we evaluated electrostatic solvation effects for two of the most frequently used solvents (benzene, $\epsilon = 2.3$, and dichloromethane, $\epsilon = 8.9$) at the B3LYP/6-31G* level with the Tomasi model (Tables 3 and 4).[17] Interestingly, transition structures **4a** and **4b** are stabilized by ~0.7−1.2 kcal/mol more than **3b**. Thus, when the calculated solvent effect is added to the gas-phase B3LYP/6-31G* free enthalpies, we can observe that in solvents of low polarity (benzene) the energy difference between the most stable *syn,endo*-**3b** and its syn,exo counterpart **4b** becomes almost negligible (Table 3) while a moderate polarity (dichloromethane) succeeds in reversing the stability order. Namely, in the latter solvent both **4b** (−0.43 kcal/mol) and **4a** (−0.19 kcal/mol) are more stable than **3b** (0.00 kcal/mol), which, however, continues to show a lower free enthalpy than **3a** (1.14 kcal/mol) (Table 3). Moreover, if the B3LYP/6-311G** gas-phase free enthalpies are used, prevalence of **4b** over **3b** already takes place in benzene and is strengthened in dichloromethane (stability order, *syn,exo*-**4b** > *syn,exo*-**4a** > *syn,endo*-**3b** > *syn,endo*-**3a**: −0.91, −0.36, 0.00, and 1.18 kcal/mol, respectively; Table 4). Finally, adding solvation effects to B3LYP/6-311+G** gas-phase free enthalpies leads to clear-cut dominance of the syn reaction channel through *exo*-**4b** (by 1.86 kcal/mol) over that one through *endo*-**3b** in dichloromethane.[26]

Solvation is also responsible for a substantial reduction of the free enthalpy difference between anti and syn TSs. For example, in dichloromethane *anti,exo*-**6a** is roughly as stable as *syn,endo*-**3a** (Table 4).

*These data clearly demonstrate that in peroxy acid epoxidation of acyclic allylic alcohols hydrogen bonding can take place at the peroxo oxygens in syn TSs (i.e., exo-**4a** and exo-**4b**) that look similar to TSs of the corresponding dioxirane epoxidations.[10a,27] Moreover, these TSs can compete on the same foot and even overcome syn TSs with C═O- - -HO (allylic) hydrogen bond (i.e., endo-**3a** and endo-**3b**).* The actual approach may well also depend on other factors, in particular, steric factors. For example, steric factors should favor TSs of the exo type (i.e., **4**) over those of the endo type (i.e., **3**) in cis-disubstituted allylic alcohols.

Another important point that emerges from calculations is that *the most stable TSs **3b** and **4b** feature a conformation for the C_1-OH bond (i.e., conformation **b**, with $O-C_1-C_2-C_3 \approx 17°$) that has rarely[28] been taken into account in qualitative TS models used for explaining face selectivity observed in acyclic allylic alcohol epoxidations.* As a rule, conformation of type **a** has been assumed in qualitative models (see **A**−**D** in Figure 1) for syn attacks. For example, it has been repeatedly stated[4b,6] that a conformation of type **a** with $O-C_1-C_2=C_3$ near 120° best accommodates the facial diastereoselectivities of these reactions.[28]

Transition structure **4a** resembles Sharpless model (i.e., **C** and **D**) but with some significant differences. In **4a**, hydrogen bonding preferentially involves the proximal oxygen atom but also the distal oxygen seems to be to some extent hydrogen bonded. More important is the observation that in **4a** the PFA plane is oriented at 101° (see γ in Table 2) to the C═C bond axis at variance with the ~60° suggested by Sharpless. Actually, the electron back-donation from the peroxy acid to the olefin is best described by the interaction between the antibonding combination of the p-type peroxo lone pairs and the π^* orbital: this interaction is at its maximum for a perpendicular orientation of the PFA plane to the C═C bond axis (i.e., **G**, Figure 1).[2b,10b−c,30]

In the case of cyclobutenol, conformations of type **b** and **e** (with O−C−C−C close to 0°) cannot be attained, and hydrogen-bonded conformation **2a** prevails over **2c** and **2d**. Only two syn TSs, namely *syn,endo*-**7a** and *syn,exo*-**8a** (which are strictly related to *syn,endo*-**3a** and *syn,exo*-**4a**), were located for the reaction of PFA with **2** in addition to six anti TSs (only those with conformation **a**, i.e., *anti,endo*-**9a** and *anti,exo*-**10a**, are here reported).[22]

Inspection of the geometries of the two syn TSs show that in *syn,endo*-**7a** the stronger hydrogen bonding (in **7a** the allylic OH stretching frequency is the lowest of all the TSs) is once again accompanied by distortion in the PFA fragment and by a worse trajectory of approach of the two reactants (as inferred, for example, from comparison with the geometry of the related *anti,endo*-**9a**). In contrast, hydrogen bonding in *syn,exo*-**8a** takes place comfortably in absence of significant structural anomalies. Moreover, a widening (by ≥4°) in the $O-C_1-C_2-C_3$ torsional angle in *syn,endo*-**7a**, in comparison with the same angle in the other three TSs (Table 2) and in the starting cyclobutenol (Table 1), testifies to the presence of further strain that destabilizes this TS.

It should be emphasized that in *syn,exo*-**8a**, a Sharpless-type TS, the PFA plane is oriented at 82° to the $C_2=C_3$ bond axis and that this value seems to be a lower

(25) Also at the B3LYP/6-311+G** level TS **4b** is favored over **3b** by entropy factors (2.2 eu).

(26) Solvation energies calculated with the AMSOL method (in cyclohexane, $\epsilon = 2.02$) confirm the results of the Tomasi method (in benzene, $\epsilon = 2.30$). See Tables 4 and 13 of the Supporting Information. After solvent effect is added to the B3LYP/6-31G* (B3LYP/6-311G**) data, the relative free enthalpies for **4b**, **3b**, **4a**, **3a**, **6a**, and **5a** are as follows: −0.16, 0.00, 0.34, 1.83, 1.97, 2.70 (−0.64, 0.00, 0.17, 1.87, 1.66, 2.74) kcal/mol.

(27) The $O-C_1-C_2-C_3$ dihedral angle in *syn,exo*-**4a** and *syn,exo*-**4b** exhibits a very similar value to that in the corresponding TSs for dimethyldioxirane epoxidation of propenol (i.e., 135.0° vs 135.9° and 16.0° vs 20.8°, respectively).

(28) (a) Chautemps, P.; Pierre, J. L. *Tetrahedron* **1976**, *32*, 549. (b) Also, Evans et al. (see ref 3, p 1319) seem to have considered conformation of type **b**, i.e., in the transition structure aimed at explaining the cooperative hydrogen-bonding interactions with the attacking peroxy acid of an allylic OH group and of a homoallylic ether group in the alkene.[29] Evans et al. corrected the model proposed by Kishi et al. (which displays a conformation of type **a** with hydrogen bonding between the OH group and the distal peroxo oxygen of the peroxy acid)[29] by suggesting a conformation of type **b** (with O−C−C═C ≈ 30°) wherein the alkene hydroxylic proton hydrogen bonds the proximal peroxo oxygen of the peroxy acid. In both models the peroxy acid proton hydrogen bonds the homoallylic ether.

(29) Johnson, M. R.; Kishi, Y. *Tetrahedron Lett.* **1979**, 4347.

(30) A perfect "perpendicular" spiro geometry with both $\gamma = 90°$ and $\delta = 90°$ is intrinsically favored in epoxidation with peroxy acid. However, the system seems to resist more to deviate from $\delta = 90°$ than from $\gamma = 90°$. Actually deviations of δ values from 90° are less than 7° for all the TSs reported in Table 2. In the case of γ deviations from 90° are less than ~10° for Sharpless-like exo TSs, but much larger distortions (even by >30°) were observed for endo orientations. That is, TSs of peroxy acid epoxidation exhibit a high flexibility as far as the γ parameter is concerned: large deviations from 90°, which allow the system to accommodate steric interactions and to strengthen hydrogen bonding, do not give rise to prohibitive energy increase. The potential energies surface is flat in the region of the TS with respect to the motion described by γ.

limit for this angle for peroxy acid epoxidation. Actually, calculations in progress in our laboratories on the PFA epoxidation of 2-cyclohexen-1-ol indicate a value of ~95° for this angle (i.e., γ) in syn TSs. Thus, an almost perpendicular orientation of the peroxy acid plane to the C=C bond axis (i.e, with γ in the range ~80−100°) is a geometry feature that must be included in Sharpless-type TSs.[30]

Data gathered in Tables 3 and 4 illustrate that the syn,exo TS with hydrogen-bonded peroxo oxygens, i.e., **8a**, always has a noticeably lower energy than its syn,endo counterpart with a hydrogen bond at the carbonyl oxygen, i.e., **7a**. The difference in stability progressively increases on extending the basis set as well as on going from gas phase to solution, to finally get the remarkable value of 3.0 kcal/mol in CH_2Cl_2. No doubt the presence of two cis substituents gives rise to significantly larger steric crowding in *syn*,*endo*-**7a** with respect to its syn,exo counterpart **8a** (in free enthalpy terms it should be of the order of ≥1.6 kcal/mol, as judged from the free enthalpy difference between *anti*,*exo*-**10a** and *anti*,*endo*-**9a**), thus strongly contributing to the higher stability of the latter over the former.

Also, *anti*,*exo*-**10a**, while less stable (by 1.76 kcal/mol) in the gas phase, becomes more stable (by 0.76 kcal/mol) than *syn*,*endo*-**7a** in moderately polar solvents (dichloromethane).

The data reported in this section provide compelling computational evidence that in the epoxidation of cyclic allylic alcohols reaction pathways via TSs with hydrogen bonding to the peroxy acid peroxo oxygens (i.e., ***8a*** *and* ***10a****) are not only viable but also favored reaction channels.*

Conclusion

A reasonable generalization of our data is as follows: all the reaction pathways via syn TSs of type **3**−**4** (with hydrogen bonding to either carbonyl oxygen or peroxo oxygens) can compete with each other in the epoxidation of acyclic allylic alcohols, and a delicate balance of effects can lead to dominance of one of them over the others. Anti TSs of type **5**−**6**, although intrinsically less favored than syn TSs, might well come into play in polar solvents.

"Spiro-butterfly" syn,exo (with hydrogen bonding interaction involving the peroxo oxygens, e.g., **8a**) and anti,exo (e.g., **10a**) TSs lend themselves as the more appropriate models to discuss facial selectivity in peroxy acid epoxidation of cyclic allylic alcohols.

TSs **4a** and **8a** closely resemble the Sharpless peroxy acid epoxidation model, i.e., **C**−**D**. This transition structure can be retained as a simple and useful model with the additional assumption that the peroxy acid plane and the C=C bond axis are almost perpendicular to each other (i.e., $\gamma \approx 60°$ in **D** must be replaced by $\gamma \approx 90°$).

Acknowledgment. Financial support from MURST and CNR is gratefully acknowledged.

Supporting Information Available: Electronic energies, activation parameters (gas phase and solution) and coordinates of all transition structures reported. This material is available free of charge via the Internet at http://pubs.acs.org.

JO981743U